Hindawi
Wireless Communications and Mobile Computing
Volume 2022, Article ID 3763555, 9 pages
https://doi.org/10.1155/2022/3763555

Research Article

Bidirectional CPW Fed Quad-Band DRA for WLAN/WiMAX Applications

Assad Iqbal,[1] Owais Owais,[1] Mohammed K. A. Kaabar,[2,3] Mustafa Shakir,[4] Inam Ullah,[5] Aftab Ahmad Khan,[1] Abd Ullah Khan,[6] and Ateeq Ur Rehman[7]

[1]*Department of Electrical and Computer Engineering, COMSATS University, Abbottabad, K.P.K, Pakistan*
[2]*Gofa Camp, Near Gofa Industrial College and German Adebabay, Nifas Silk-Lafto, 26649 Addis Ababa, Ethiopia*
[3]*Institute of Mathematical Sciences, Faculty of Science, University of Malaya, Kuala Lumpur 50603, Malaysia*
[4]*Department of Electrical Engineering, Superior University, Lahore 54000, Pakistan*
[5]*College of Internet of Things (IoT) Engineering, Hohai University, Changzhou Campus, 213022, China*
[6]*Department Computer Science, National University of Science and Technology, Quetta Balochistan, Pakistan*
[7]*Department of Electrical Engineering, Government College University Lahore, Lahore 54000, Pakistan*

Correspondence should be addressed to Mohammed K. A. Kaabar; mohammed.kaabar@wsu.edu, Inam Ullah; inam.fragrance@gmail.com, and Ateeq Ur Rehman; ateeq.rehman@gcu.edu.pk

Received 5 January 2022; Revised 9 May 2022; Accepted 20 May 2022; Published 3 June 2022

Academic Editor: Chunqiang Hu

Due to the size constraint, antennas with compact size are required that can support multibands with single radiating element. Dielectric resonator antenna (DRA) can support multiple modes with good efficiency and gain using single radiating element. In this paper, a quad-band DRA is proposed for WLAN/WiMAX bands using a single CPW feed. Out of four bands, WLAN (2.37-2.55) GHz, (5.15-5.35) GHz, and (5.6-5.83) GHz are achieved by the excitation of fundamental and higher-order modes whereas WiMAX (3.58-3.72) GHz band is achieved by dielectric loading of the DR. Dielectric loading makes it possible to operate the antenna at desired frequency band. Due to the partial ground plane and single coplanar waveguide (CPW) feed radiation pattern of the proposed antenna is bidirectional. The design is efficient in terms of radiation efficiency. Simulated and measured results show that it can be a suitable candidate for WLAN and WiMAX applications.

1. Introduction

The advance wireless communication technologies are expected to support massive devices with low energy consumption and high spectral efficiency [1, 2]. These technologies are backscatter communications, multiple input and multiple output, device-to-device communication, vehicular communication, non-orthogonal multiple access (NOMA), Internet of things (IoT), cognitive radio, artificial intelligence, smart drones, reconfigurable intelligent surfaces, and so on. More specifically, the authors of [3] have introduced NOMA to Internet of vehicles network to maximize the total achievable energy efficiency of the system. Moreover, authors in [4] provided a new framework for spectrum and energy efficiency of NOMA network and investigated energy efficiency of vehicular network. The authors of [5] proposed reinforcement learning for blockchain networks. The work in [6] has investigated the energy efficiency of IoT networks. In addition, the work of [7] has studied the performance of drones while [8] has presented device-to-device communication in NOMA network. Of late, [9, 10] have investigated spectral efficiency and energy efficiency using single objective and multiobjective approaches. However, there exist several challenges in these technologies that need to be investigated. For example, designers are focusing on the miniaturization of devices as technology advances. Besides that, there is also an increase in the number of applications, which necessitates the use of various spectrums such as microwave, millimeter wave, and terahertz bands. Moreover, multiple antennas can be used to meet high data rate demands and provide reliable communication. As mutual coupling increases, it becomes

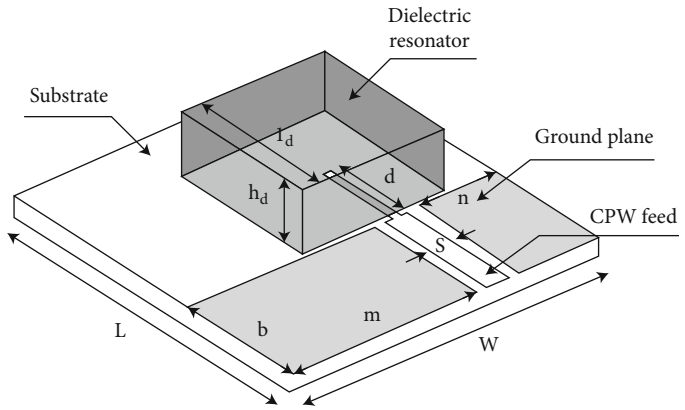

Figure 1: Geometry of the proposed DRA showing all elements of the DRA.

Table 1: Dimension of the proposed antenna design.

Variable used	Value (mm)	Variable used	Value (mm)	Variable used	Value (mm)
W	33	L	34	h_s	1.5
h_g	0.017	h_d	6	a	1
m	20	n	8.5	s	2.5
g	1	b	13	w_d	15
l_d	15	c	0.5	d	9
k	5.5	ε_s	4.4		

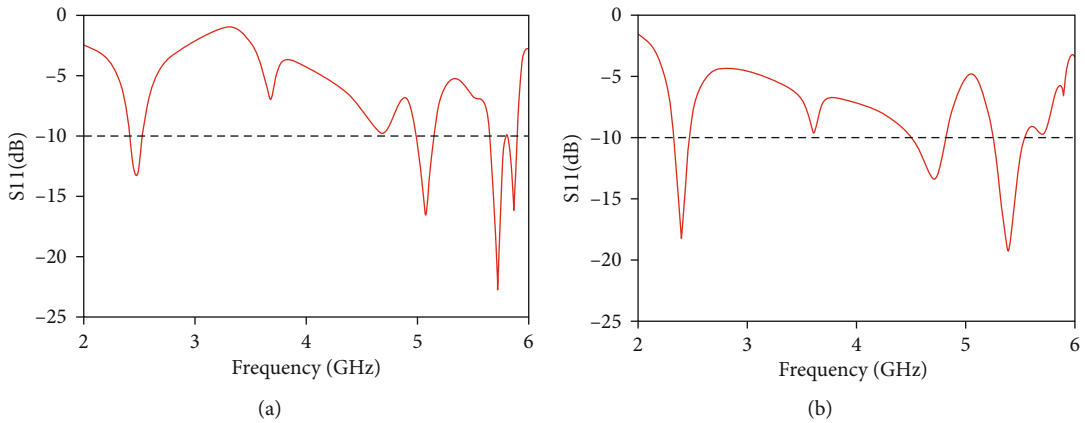

Figure 2: S-parameters due to variation in CPW strip length. (a) Strip length increased. (b) Strip length decreased.

more difficult for design engineers to incorporate a large number of antennas in small devices. Although compact single reconfigurable metallic elements cannot provide enough bandwidth, DRA has a wider impedance bandwidth at high frequencies than metallic antennas [11].

Since the last few years, the DRAs have gained more consideration due to various features like high radiation efficiency, wider impedance bandwidth, high gain, and low metallic losses as compared to metallic antennas such as microstrip patch antennas (MPAs) and planar inverted F-antenna (PIFAs). DRA has been recommended and developed for use in microwave and millimeter-wave frequency bands. Compared with microstrip patch antennas (MPA) that have discovered a wide range of applications [12]. Moreover, DRA can easily be excited by multiple feeding techniques such as coplanar waveguide, coaxial probe, hybrid feeding, and aperture coupling [13]. As compared with MPA, the DRA has a much more extensive impedance bandwidth (~10% for dielectric constant $\varepsilon r \sim 10$). This is because the microstrip antenna radiates just through two narrow radiation slots; however, the DRA radiates through its entire surface except the grounded part. Avoidance of the surface waves is one of the advantages of the DRA over the microstrip antenna. In any case, numerous attributes of the DRA and microstrip antenna (MA) are common because they

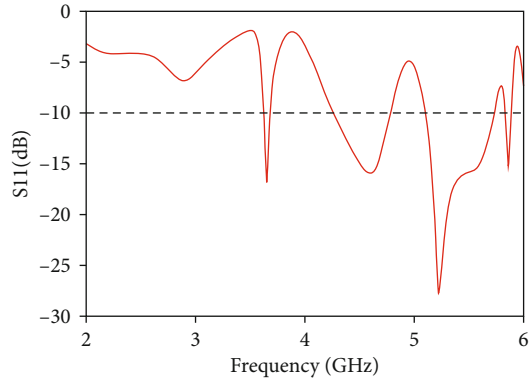

Figure 3: Effect of variation in ground plane width on S-parameters.

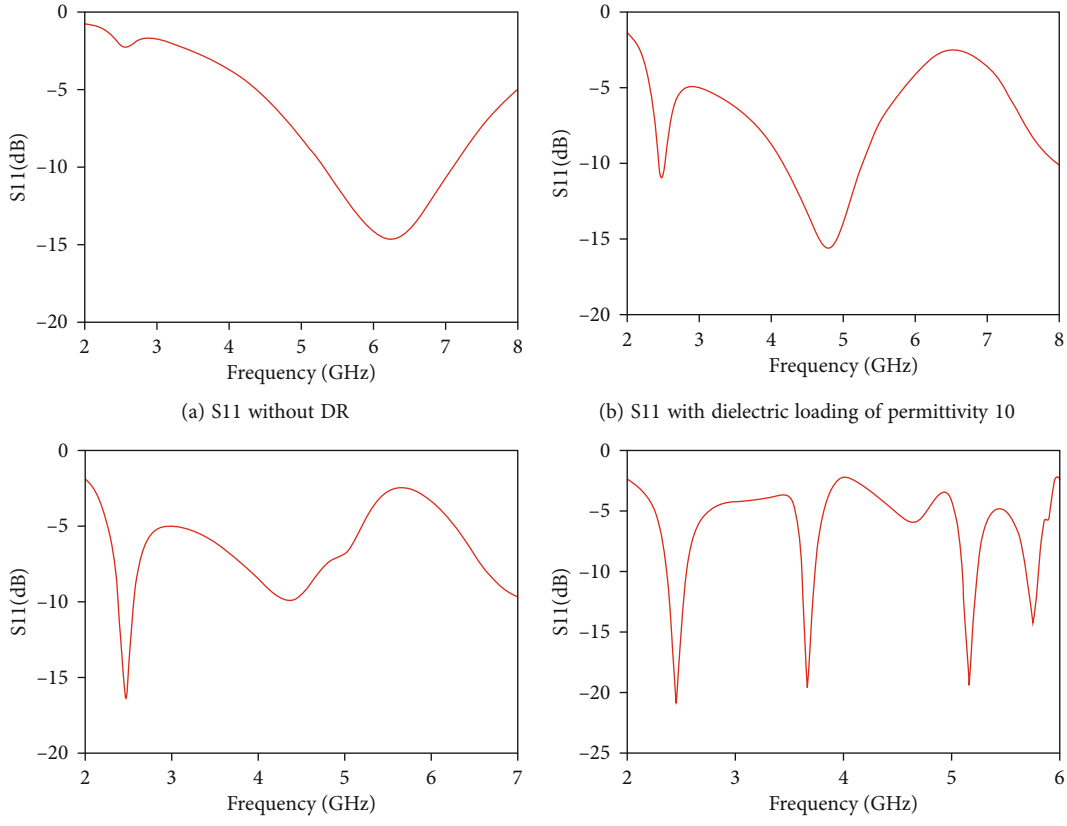

(a) S11 without DR

(b) S11 with dielectric loading of permittivity 10

(c) S11 with dielectric loading of permittivity 20

(d) S11 with dielectric loading of permittivity 30

Figure 4: Effect of loading with different permittivity material on S-parameters.

behave like resonant cavities. Besides, practically all the excitation methods that are applied to the MA can be utilized for the DRA. A detailed explanation of DRA with almost all aspects like its shapes, feeding mechanism, radiation patterns, and modes can be found in [14].

Recently, it has been investigated that various applications are working at different frequency bands; so, it is not viable to design an antenna for each application separately because of the increase in cost and size of the device [15]. Therefore, it is advantageous to design a multiband antenna with a single structure to reduce the cost, size, and complexity of the system [16–19]. It is the property of DRA that it can excite multiple modes using a single DR structure when excited by a suitable feeding structure [20]. Therefore, the feeding mechanism plays an important role to excite required mods in the DRA. In different papers, different feeding techniques such as microstrip line, coaxial probe, and CPW feed are used to excite multiple modes in DRA [21–24]. In some cases, pentagon and hexagon shapes of feeding structures have been used to achieve multiple bands [25]. In [26], Hamsakutty et al. achieved a triple band by using two segments of rectangular DRA, which make the overall structure bulky. In [27], the authors used segmented DRA to

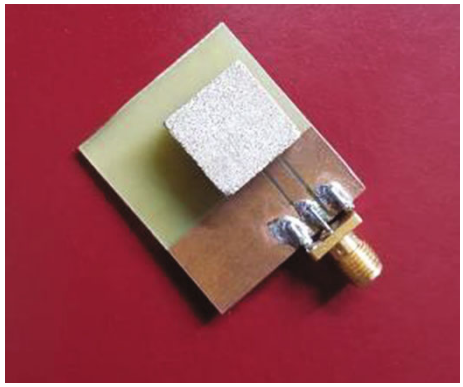

Figure 5: The prototype of the proposed quad-band DRA.

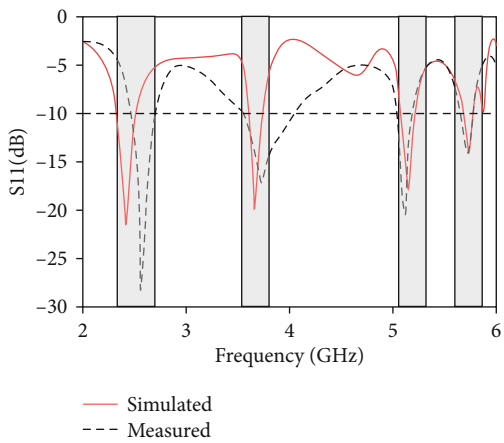

Figure 6: Measured and simulated S11 at all four bands.

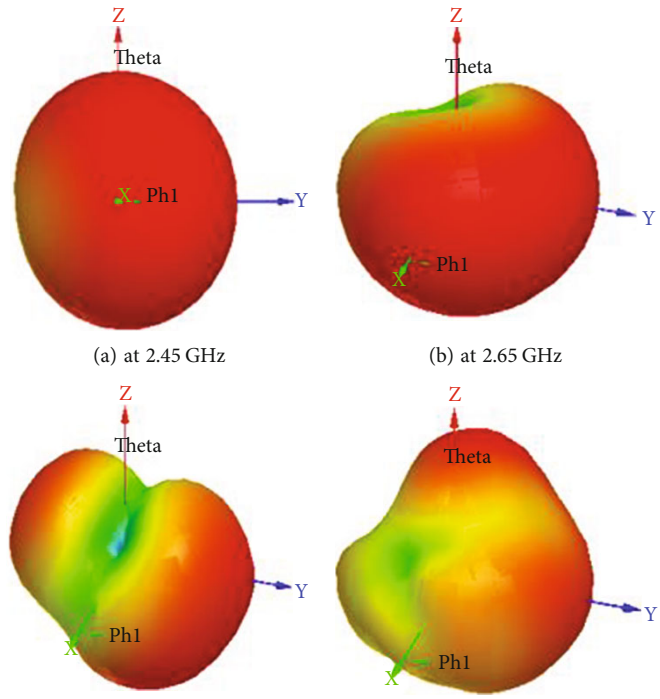

Figure 7: Three dimensional radiation patterns of the DRA.

achieve triple bands; however, they used complex feeding which ultimately complicates the fabrication process. In [28], Sharma and Gangwar proposed a triple-band hybrid DRA for 4G LTE application. In this work, two bands are achieved through feed line and higher-order modes. A unidirectional radiation pattern at all three bands is achieved in this design. For particular services where users move in a straight path like highways, tunnels and railways bidirectional antennas are more useful to maximize the link efficiency [29, 30]. In [31], two unidirectional antennas in the opposite direction have been used for bidirectional radiation pattern; however, the design was complicated and directivity was also low. A bidirectional radiation pattern has also been achieved with antennas having more than one feeding mechanism [32].

Multiple techniques have been used to design multiple-band DRAs, which are the subject of this section's investigation. The author of paper [33] achieved a triple-band by simultaneously exciting the four DR arrays. The proposed design operates at frequencies ranging from 0.86 to 1.04 GHz, 2.37 to 2.79 GHz, and 4.17 to 5.21 GHz. The array of four DR increases the overall size of the antenna while also making it bulky, making installation of such antennas in modern wireless gadgets difficult. In paper [33], the authors designed a triple-band dielectric resonate antenna by exciting two DR segments. The first two bands are achieved by exciting the two DR via feed line, and the third band is achieved through reconfigurability. Because switches are used for reconfigurability, the design of this DRA is extremely complicated. Because two DR segments are used, the overall design of this DRA is bulky. A star-shaped DR was excited by a simple microstrip feed line in paper [22], and the proposed design covered three frequency bands of 5.04 –6.13 GHz, 6.87 –7.97 GHz, and 8.58 –9.63 GHz. The construction of such an antenna is extremely difficult. This design's radiation pattern is unidirectional. Furthermore, the authors of the paper [34] designed a multiband DRA. The multiband is achieved in this design by exciting two cylindrical DR and two C shape patches. Because of the lack of a bottom ground structure, the radiation pattern of this design is bidirectional, which increases the size of the antenna of the whole communication system. A triple-band dielectric resonates antenna with operating frequencies of 1.8 GHz, 2.2 GHz, and 2.6 GHz was also designed and investigated [35]. There is no fabrication involved in this design, and the results are calculated. Only simulated results were shown by the author. The design has a substantial overall size.

Most of the DRAs listed above have multiple resonating elements, which are either very complicated to design or mostly support dual-band or triple-band operation. As a result, in this paper, a single square-shaped DR was excited via a CPW feed line. The proposed design has no bottom ground plane due to which the radiation pattern of the antenna becomes bidirectional, the operating band of the proposed design is WLAN (2.37-2.55) GHz, (5.15-5.35) GHz, (5.6-5.83) GHz, and WiMAX (3.58-3.72). Both WiMAX and WLAN bands can serve hundreds of users with a speed of 10 Mbps at 10 km with a line of sight. The use of these bands has been increased with

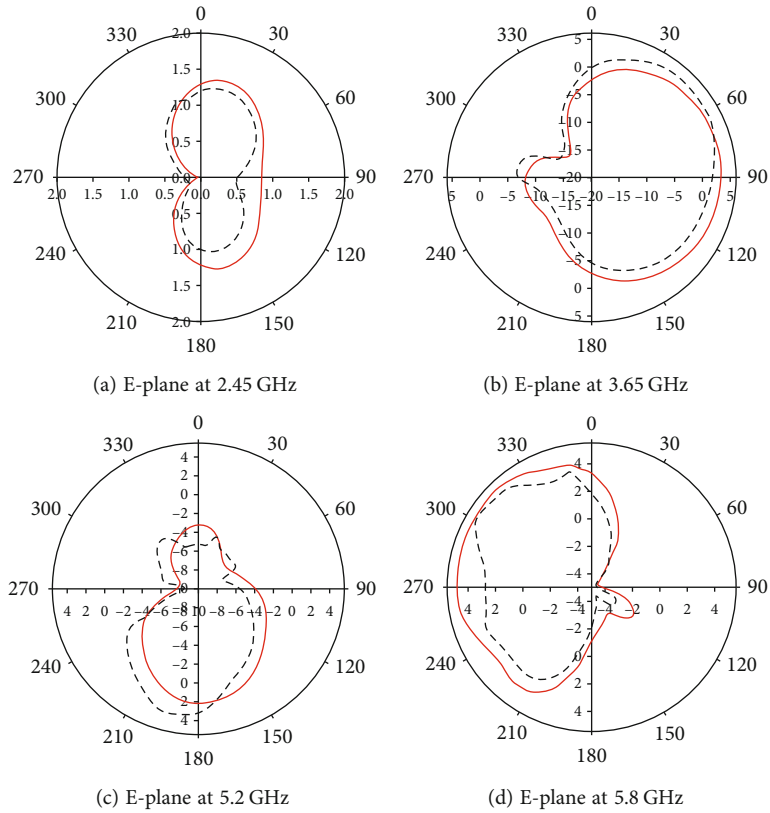

(a) E-plane at 2.45 GHz

(b) E-plane at 3.65 GHz

(c) E-plane at 5.2 GHz

(d) E-plane at 5.8 GHz

Figure 8: Simulated and measured E-planes.

the advent of applications with multiband support. From the comparison table, the size of the proposed design is much smaller than other DRAs, which compact and miniaturize the size of modern wireless communication devices.

In this paper, bidirectional radiation patterns have been achieved for four bands using single radiating elements with a single feeding structure. The rectangular DRA has no ground plane at the bottom which makes its radiation pattern bidirectional. It covers three bands including WiMAX and WLAN. Moreover, a quad-band DRA is proposed and achieved for WLAN/WiMAX bands using a single CPW feed. Bidirectional radiation pattern is achieved at all radiating element.

The remaining paper is organized as below: the antenna design parameters and analysis are described in Section 2. Section 3 presents the parametric study, while Section 4 presents the results and discussion. Finally, Section 5 concludes this work.

2. Antenna Design and Analysis

Figure 1 shows the geometry of the proposed DRA. Dimensions of the DR is $[l_d \times (w_d = l_d) \times h_d]\,\text{mm}^3$ placed on FR4 substrate with permittivity ε_s and height h_s. The DRA is excited through CPW feed line with optimized impedance matched at 50Ω. In order to improve the impedance matching of DR with CPW feed, a stub of width 1 mm is also added at the end of the coplanar feed. Table 1 summarizes the optimized values of the proposed DRA.

3. Parametric Study

The parametric study comprised of variation of CPW feeds on resonant frequencies with and without loading of DR on the substrate.

3.1. Variation without DR Loading. Resonant frequencies of the proposed design depend on the length of the CPW strip. If the length of the strip is increased beyond 9 mm, it is clear from Figure 2(a) that the impedance matching and bandwidth impedance of the lower WLAN band (2.45 GHz) are decreased. Impedance matching and bandwidth of the remaining two bands remain the same. If the length of CPW feed is decreased below 9 mm; the resonance of the lower band remains unaltered but resonances of the upper two bands from 5.1 GHz to 4.7 GHz and from 5.8 GHz to 5.6 GHz. This phenomenon is shown in Figure 2(b). However, it still does not fulfill the requirements of WLAN bands as it has very poor impedance matching as well.

Resonance frequencies also depend upon the width of the ground plane. When the width of the ground plane is decreased below 13 mm, it is clear from Figure 3 that the proposed design has no resonance at 2.45 GHz, and the impedance bandwidth of the WiMAX band is also decreased.

The resonance frequencies are also reliant on the width of the ground plane, and if the width of the ground plane is decreased from 13 mm, it is clear from Figure 3 that the proposed design has no resonance at 2.45 GHz, which has been achieved by DR loading.

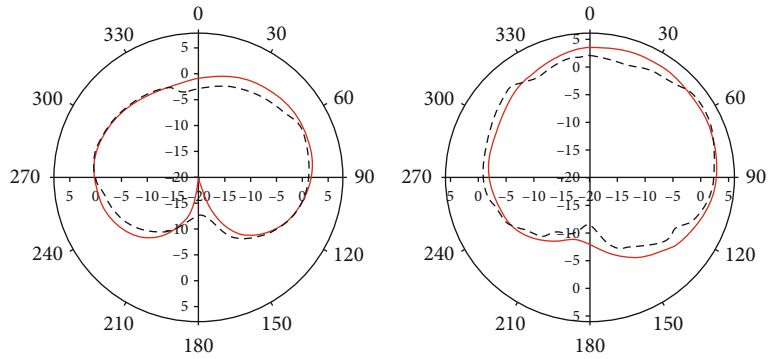

(a) H-plane at 2.45 GHz

(b) H-plane at 3.65 GHz

(c) H-plane at 5.2 GHz

(d) H-plane at 5.8 GHz

Figure 9: Simulated and measured H-planes.

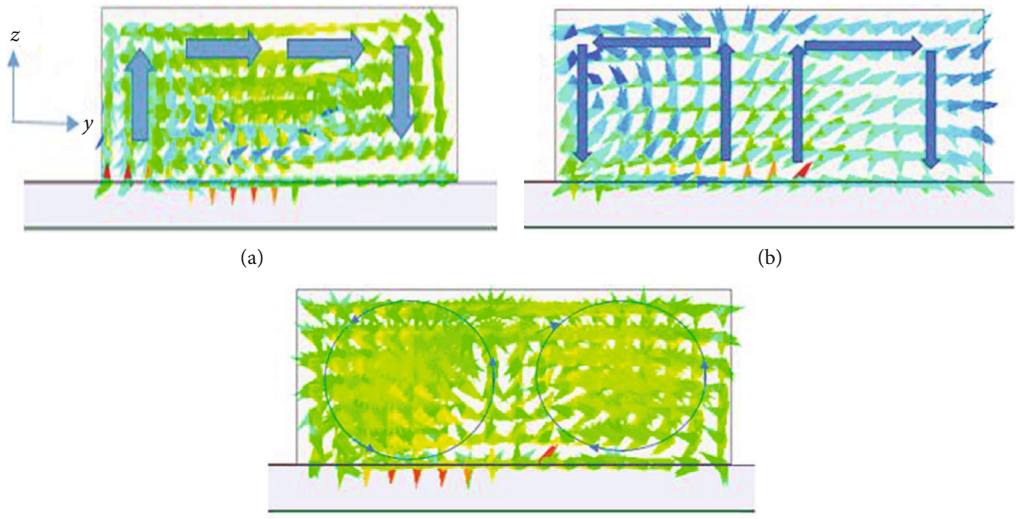

(a)

(b)

(c)

Figure 10: TE modes. (a) TE_{111}. (b) TE_{121}. (c) TE_{142}.

3.2. Variation with DR Loading. The dielectric loading effect is inversely proportional to the resonance frequency. It is clear from Figure 4(a) that without dielectric loading, DRA resonates at 6.2 GHz. Due to the dielectric loading of DR with permittivity 10, the resonance point shifts back to 4.8 GHz, as shown in Figure 4(b). This is fundamental mode excitation in the DR, and other modes also shit accordingly. Figures 4(c) and 4(d) reveal the fundamental mode excitation for DR loading with permittivity 20 and 30, respectively. For permittivity 20, it shifts to 4.3 GHz, and for 30, shifting takes place on 3.6 GHz.

When the permittivity of the material is increased to 20, the resonance frequency of the antenna is shifted to 4.3 GHz from 4.8 GHz which is shown in Figure 4(c). When the

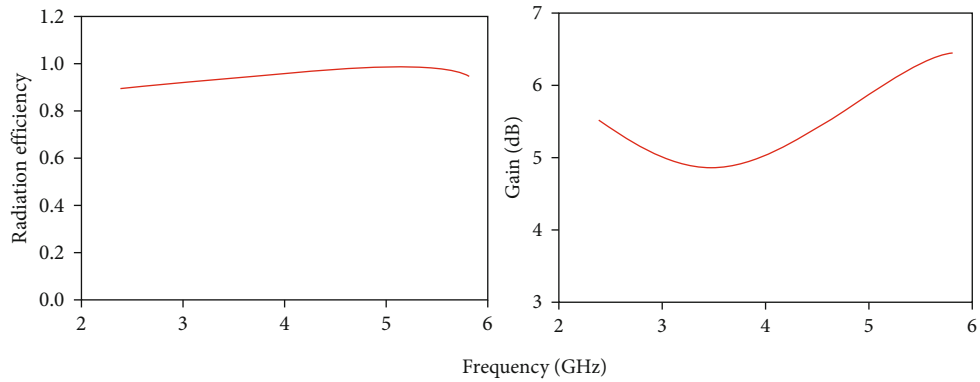

Figure 11: (a) Radiation efficiency vs. frequency. (b) Gain vs. frequency.

Table 2: Value radiation efficiency and gain are listed Table 2.

References	No. of DR element	No. of band	Gain (dBi)	Size ($L \times w \times h$) mm^3
[33]	4	3	7.2	$96 \times 113 \times 15.6$
[33]	2	3	5.2	$230 \times 134 \times 5.6$
[22]	1	3	8.10	$50 \times 50 \times 7.60$
[34]	2	4	6.5	$50 \times 50 \times 11.2$
[35]	1	2	5.3	$100 \times 70 \times 11.4$
[39]	1	3	6.86	$140 \times 140 \times 11.6$
Proposed work	1	4	6.45	$33 \times 34 \times 7.4$

Table 3: A comparison with related multiband DRAs.

Frequency (GHz)	2.45	3.65	5.25	5.81
Gain (dBi)	5.5	4.9	6.1	6.41
Rad. efficiency	0.9	0.85	0.91	0.94

material has a permittivity of 30 is loaded on CPW feed, the resonance frequency of the antenna is shifted from 4.3 GHz to 3.65 GHz, which is the required WiMAX band, the proposed design gives the resonance at 2.45 GHz is due to the excitation of the fundamental mode in DR, while resonance at 5.15 GHz and 5.8 GHz is due to the excitation of higher mode in DR which is clear from Figure 4(d).

4. Result and Discussions

This section includes the antenna and its performance parameters. First, the antenna performance parameters such as S-parameters with respect to design are described; followed by performance matrices like radiation pattern, gain, and efficiency.

Figure 5 shows the model of the proposed designed antenna. The DR has a permittivity of 30 and a tangent loss of 0.002, which is made from Eccostock® Hik500f. The ground plane is fixed on an FR4 substrate having a permittivity of 4.4 and a thickness/breadth of 1.5 mm. The DR is placed on the substrate through a glove of permittivity close to 2.

Simulated and measured S-parameters are shown in Figure 6. Shaded region in the figure shows the required band of interest. Results show that antenna is well matched at all the bands except the last band. The reason may be the ground plane size at this band because it is the higher mode excited in the DRA. Mismatch in simulated and measured results is due to the fabrication tolerances.

Figure 7 shows 3D patterns at each frequency band. It is clear from figure that direction of radiation pattern at each band is different, covering each direction at each band. This is one of the advantages of the partial ground plane. However, partial ground plane lowers the gain of the antenna due to the backlobe which is one of its drawback. A bidirectional radiation pattern with a simple structure and single feeding mechanism is achieved at all four ports. Simulated gain at all four bands is up to 6.45 dBi. It can be increased by extending the ground plane; however, this action degrades the bidirectional performance of the patterns as discussed earlier.

Figures 8 and 9 show that the simulated and measured E- and H- plane of proposed DRA, respectively. Solid line shows the simulated, and the dotted line represents the measured results. Both E and H plane of the patterns shows bidirectional radiation patterns but at the cost of backward radiations. It is clear from all the figures that the measured and simulated results are in good arrangement.

DRA can support multiple modes, and its fundamental mode depends on its aspect ratio dielectric permittivity. Aspect ratio is the ratio of length: width and length: height [36]. In the proposed work, fundamental mode in the DR is excited at 2.45 GHz as shown in Figure 10(a). This mode is TE_{111} mode, represented by a half wave of electric field pattern, showing the wave-number = $\pi/2$.

Similarly at 5.2 GHz, TE_{121} mode is excited, represented by two half waves as shown in Figure 10(b). At 5.8 GHz, TE_{142} mode has been excited. As there is no ground plane under the DR element; therefore, even mode can be excited [36]. Four half-waves in the y-axis and two half-waves in the z-axis can be seen in Figure 10(c). A complete circle represents two half-waves.

WiMAX (3.58-3.72) GHz band is achieved by dielectric loading of the DR therefore no specific pattern of the field is achieved as shown.

Figures 11(a) and 11(b) show the gain vs. frequency and radiation efficiency vs. frequency pots, respectively. It can be

seen from plots that both gain and radiation efficiency are small (4.9 and 0.85) as compared to the other values. It is because the band at 3.65 GHz is due to dielectric loading, and the remaining three bands are due to the excitation of modes in the DRA. Gain and radiation efficiency against each frequency band is shown in Table 2.

Table 3 shows the comparison of some recent research with the proposed work. It can be seen that in terms of number of DR elements, our design uses only one which results in reduced size as compared to other antennas. Moreover, the proposed design covers four bands with single CPW feed.

In this work, single CPW feed and DR element have been used to achieve bidirectional radiation pattern. This arrangement reduces the size of the antenna. This work can be extended for quad-band MIMO design for 5G applications. For this purpose, another orthogonal CPW feed can be added symmetrically to achieve quad-band MIMO in the same frequency. However, there may be the issue of isolation at each degenerate mode which can be enhanced using different techniques available in literature.

5. Conclusion

In this paper, a CPW feed bidirectional quad-band DRA is proposed for WLAN and WiMAX bands. The proposed design covers WLAN (2.37-2.55) GHz, (5.15-5.35) GHz, (5.6-5.83) GHz, and WiMAX (3.58-3.72) GHz bands. The proposed design with single feed and single DR element provides four bands with the capability of bidirectional radiation pattern. Bidirectional radiation at all four bands has been achieved using a simple design technique. The radiation efficiency of the proposed design is 94% and gains up to 6.45 dBi. This design can be used in wireless gadgets and other related applications. All the measured and simulated results of the proposed design show that it will be an appropriate candidate for WLAN and WiMAX applications.

As a future task, the proposed work can be extended for MIMO design that can be used for 5G applications. This can be done by using another CPW feed, orthogonally oriented along the same DR element. Moreover, the design can be used for quad-band array design for 5G applications.

Data Availability

The dataset used for the experiments in this study is available upon reasonable request from the corresponding author.

Conflicts of Interest

The authors declare no conflict of interest.

Authors' Contributions

Assad Iqbal did the actualization, methodology, formal analysis, software, validation, investigation, and initial draft. Owais Owais did the actualization, validation, methodology, software, formal analysis, investigation, and initial draft. Mohammed K. A. Kaabar did the actualization, methodology, formal analysis, validation, investigation, initial draft, and supervision of the original draft and editing. Mustafa Shakir did the actualization, validation, methodology, formal analysis, investigation, and initial draft. Inam Ullah did the actualization, validation, methodology, formal analysis, investigation, and initial draft. Aftab Ahmad Khan did the actualization, validation, methodology, formal analysis, investigation, and initial draft. Abd Ullah Khan did the actualization, validation, methodology, formal analysis, investigation, and initial draft. Ateeq Ur Rehman did the actualization, validation, methodology, formal analysis, investigation, and initial draft. All authors read and approved the final version.

References

[1] W. U. Khan, X. Li, A. Ihsan, M. A. Khan, V. G. Menon, and M. Ahmed, "NOMA-enabled optimization framework for next-generation small-cell IoV networks under imperfect SIC decoding," *IEEE Transactions on Intelligent Transportation Systems*, 2021.

[2] W. U. Khan, T. N. Nguyen, F. Jameel et al., "Learning-based resource allocation for backscatter-aided vehicular networks," *IEEE Transactions on Intelligent Transportation Systems*, 2021.

[3] F. Jameel, S. Zeb, W. U. Khan, S. A. Hassan, Z. Chang, and J. Liu, "NOMA-enabled backscatter communications: toward battery-free IoT networks," *IEEE Internet of Things Magazine*, vol. 3, no. 4, pp. 95–101, 2020.

[4] W. U. Khan, M. A. Javed, T. N. Nguyen, S. Khan, and B. M. Elhalawany, "Energy-efficient resource allocation for 6G backscatter-enabled NOMA IoV networks," *IEEE Transactions on Intelligent Transportation Systems*, 2021.

[5] F. Jameel, U. Javaid, W. U. Khan, M. N. Aman, H. Pervaiz, and R. Jäntti, "Reinforcement learning in blockchain-enabled IIoT networks: a survey of recent advances and open challenges," *Sustainability*, vol. 12, no. 12, article 5161, 2020.

[6] W. U. Khan, F. Jameel, M. A. Jamshed, H. Pervaiz, S. Khan, and J. Liu, "Efficient power allocation for NOMA-enabled IoT networks in 6G era," *Physical Communication*, vol. 39, article 101043, 2020.

[7] S. K. Haider, A. Jiang, A. Almogren et al., "Energy efficient UAV flight path model for cluster head selection in next-generation wireless sensor networks," *Sensors*, vol. 21, no. 24, article 8445, 2021.

[8] S. Yu, W. U. Khan, X. Zhang, and J. Liu, "Optimal power allocation for NOMA-enabled D2D communication with imperfect SIC decoding," *Physical Communication*, vol. 46, article 101296, 2021.

[9] W. U. Khan, J. Liu, F. Jameel, V. Sharma, R. Jantti, and Z. Han, "Spectral efficiency optimization for next generation NOMA-enabled IoT networks," *IEEE Transactions on Vehicular Technology*, vol. 69, no. 12, pp. 15284–15297, 2020.

[10] W. U. Khan, F. Jameel, G. A. S. Sidhu, M. Ahmed, X. Li, and R. Jantti, "Multiobjective optimization of uplink NOMA-enabled vehicle-to-infrastructure communication," *IEEE Access*, vol. 8, pp. 84467–84478, 2020.

[11] M. Abedian, S. K. A. Rahim, S. Danesh, S. Hakimi, L. Y. Cheong, and M. H. Jamaluddin, "Novel design of compact UWB dielectric resonator antenna with dual-band-rejection characteristics for WiMAX/WLAN bands," *IEEE Antennas Wireless Propagation Letters*, vol. 14, pp. 245–248, 2015.

[12] A. A. Khan, M. H. Jamaluddin, S. Aqeel, J. Nasir, J. U. R. Kazim, and O. Owais, "Dual-band MIMO dielectric resonator

antenna for WiMAX/WLAN applications," *IET Microwaves, Antennas & Propagation*, vol. 11, no. 1, pp. 113–120, 2017.

[13] S. Danesh, S. K. A. Rahim, and M. Khalily, "A wideband trapezoidal dielectric resonator antenna with circular polarization," *Progress In Electromagnetics Research*, vol. 34, pp. 91–100, 2012.

[14] K. M. Luk and K. W. Leung, *Dielectric Resonator Antenna*, Research Studies tablePress, U. K., 2003.

[15] Y. Gao, B. L. Ooi, W. B. Ewe, and A. P. Popov, "A compact wideband hybrid dielectric resonator antenna," *IEEE Microwave and Wireless Components Letters*, vol. 16, no. 4, pp. 227–229, 2006.

[16] S. Aqeel, M. R. Kamarudin, A. A. Khan et al., "A compact frequency reconfigurable hybrid DRA for LTE/Wimax applications," *International Journal of Antennas and Propagation*, vol. 2017, Article ID 3607195, 13 pages, 2017.

[17] I. Khan, Y. B. Tian, I. Ullah, M. M. Kamal, H. Ullah, and A. Khan, "Designing of E-shaped microstrip antenna using artificial neural network," *International Journal of Computing, Communications and Instrumentation Engineering*, vol. 5, no. 1, 2018.

[18] R. Khan, Q. Yang, I. Ullah et al., "3D convolutional neural networks based automatic modulation classification in the presence of channel noise," *IET Communications*, vol. 16, no. 5, pp. 497–509, 2021.

[19] W. U. Khan, N. Imtiaz, and I. Ullah, "Joint optimization ofNOMA-enabled backscatter communications for beyond5G IoTnetworks," *Internet Technology Letters*, vol. 4, no. 2, article e265, 2021.

[20] A. Ahmad Khan, R. Khan, S. Aqeel, J. Ur Rehman Kazim, J. Saleem, and M. K. Owais, "Dual-band mimo rectangular dielectric resonator antenna with high port isolation for LTE applications," *Microwave and Optical Technology Letters*, vol. 59, no. 1, pp. 44–49, 2017.

[21] V. Hamsakutty, A. V. Praveen Kumar, G. Bindu et al., "A multifrequency coaxial-fed metal coated dielectric resonator antenna," *Microwave and Optical Technology Letters*, vol. 47, no. 6, pp. 573–575, 2005.

[22] L. Huitema, M. Koubeissi, M. Mouhamadou, E. Arnaud, C. Decroze, and T. Monediere, "Compact and multiband dielectric resonator antenna with pattern diversity for multistandard mobile handheld devices," *IEEE Transactions on Antennas and Propagation*, vol. 59, no. 11, pp. 4201–4208, 2011.

[23] L. Ali, C. Wang, I. Ullah et al., "Design and optimization of microwave sensor for the non-contact measurement of pure dielectric materials," *Electronics*, vol. 10, no. 24, article 3057, 2021.

[24] I. Khan, Y. B. Tian, H. Vllah, S. U. Rahman, and M. M. Kamal, "Design annular ring microstrip antenna based on artificial neural network," in *2018 2nd IEEE Advanced Information Management, Communicates, Electronic and Automation Control Conference (IMCEC)*, pp. 2033–2037, Xi'an, Shaanxi China, May 2018.

[25] M. M. Kamal, I. Ullah, A. Ashraf, and N. Ullah, "Designing band notch features in ultra-wideband antenna," in *2017 7th IEEE International Symposium on Microwave, Antenna, Propagation, and EMC Technologies (MAPE)*, pp. 92–95, Xi'an Shi, China, October 2017.

[26] V. Hamsakutty, A. V. Praveen Kumar, J. Yohannan, G. Bindu, and K. T. Mathew, "Coaxial fed hexagonal dielectric resonator antenna for multifrequency operation," *Microwave and Optical Technology Letters*, vol. 48, no. 5, pp. 878–880, 2006.

[27] M. Bemani, S. Nikmehr, and H. Younesiraad, "A novel small triple band rectangular dielectric resonator antenna for WLAN and WiMAX applications," *Journal of Electromagnetic Waves and Applications*, vol. 25, no. 11-12, pp. 1688–1698, 2011.

[28] A. Sharma and R. K. Gangwar, "Triple band two-segment cylindrical dielectric resonator antenna with a novel microstrip feed for WLAN/WIMAX applications," *Microwave and Optical Technology Letters*, vol. 57, no. 11, pp. 2649–2655, 2015.

[29] A. Carton, C. G. Christodoulou, C. Dyck, and C. Nordquist, "Investigating the impact of carbon contamination on RF MEMS reliability," in *2006 IEEE Antennas and Propagation Society International Symposium*, pp. 1193–1196, Albuquerque, NM, USA, July 2006.

[30] H. Arai, K. Kohzu, T. Mukaiyama, and Y. Ebine, "Bi-directional notch antenna with parasitic elements for tunnel booster system," *Antennas and Propagation Society International Symposium*, vol. 4, pp. 2218–2221, 1997.

[31] A. Batgerela, J. I. Choib, and S. Y. Eomb, "High-gain bidirectional MDAS antenna design excited by stacked-microstrip dipole," *Journal of Electromagnetic Waves and Applications*, vol. 26, no. 11-12, pp. 1412–1422, 2012.

[32] T. Jia and X. Li, "A compact stacked bidirectional antenna for dual-polarized WLAN applications," *Progress In Electromagnetics Research*, vol. 44, pp. 95–108, 2013.

[33] A. Vahora and K. Pandya, "Triple band dielectric resonator antenna array using power divider network technique for GPS navigation/bluetooth/satellite applications," *International Journal of Microwave and Optical Technology*, vol. 15, pp. 369–378, 2020.

[34] P. R. Girjashankar and T. Upadhyaya, "Surface mountable multiband dielectric resonator antenna for wireless communication systems," *Progress In Electromagnetics Research M*, vol. 103, pp. 173–183, 2021.

[35] A. Sharma and R. K. Gangwar, "Circularly polarised hybrid Z-shaped cylindrical dielectric resonator antenna for multiband applications," *IET Microwaves, Antennas & Propagation*, vol. 10, no. 12, pp. 1259–1267, 2016.

[36] X. S. Fang and K. W. Leung, "Designs of single-, dual-, wideband rectangular dielectric resonator antennas," *IEEE Transactions on Antennas and Propagation*, vol. 59, no. 6, pp. 2409–2414, 2011.